Available online at www.sciencedirect.com
ScienceDirect
Journal of Power Sources 163 (2006) 357–363
JOURNAL OF POWER SOURCES
www.elsevier.com/locate/jpowsour

Effect of carbon loading in microporous layer on PEM fuel cell performance

Sehkyu Park, Jong-Won Lee, Branko N. Popov *

Center for Electrochemical Engineering, Department of Chemical Engineering, University of South Carolina, Columbia, SC 29208, USA

Received 10 July 2006; received in revised form 18 August 2006; accepted 15 September 2006
Available online 27 October 2006

Abstract

The effect of carbon loading in the microporous layer on the PEM fuel cell performance was investigated using mercury porosimetry, electrochemical polarization techniques and electrochemical impedance spectroscopy. When air was used as an oxidant, a maximum fuel cell performance was obtained for a carbon loading of 0.5 mg cm^{-2}. The ac-impedance properties were analyzed based on the thin film/flooded-agglomerate dynamics in the catalyst layer and the oxygen diffusion kinetics in the gas diffusion layer. The ac-impedance study indicated that the optimized microporous layer results in an effective water management (i.e. a balancing of water saturations in the catalyst layer and the gas diffusion layer), thereby improving the oxygen diffusion kinetics.

Keywords: Proton exchange membrane fuel cell; Gas diffusion layer; Microporous layer; Carbon loading; Water management

1. Introduction

Proton exchange membrane fuel cells (PEMFCs) are promising alternative power sources for automotive and stationary applications. The PEMFC should operate at a relatively high current density in order to achieve the highest power output. A gas diffusion layer (GDL) sandwiched between the catalyst layer and the flow field permits gas transport towards the catalyst layer from the flow field. The GDL is usually treated with hydrophobic agents to allow an effective removal of liquid water produced at the cathode catalyst [1,2].

The GDL typically has a dual-layer structure, as illustrated in Fig. 1 [3]. The first layer is a carbon-fiber cloth or paper which serves as a current collector and as a physical support for the electrode. The thinner microporous layer (MPL) consists of carbon black powder and a hydrophobic agent. It has been reported [4–8] that the MPL increases the catalyst utilization and the overall fuel cell performance depending on its structure. For instance, Lin and Nguyen [8] tested three different types of commercially available GDLs: bare SGL SIGRACET and Toray TGPH carbon-fiber papers and SGL SIGRACET carbon-fiber papers coated with the MPL. They showed that higher fuel cell performance was obtained using the MPL-coated carbon-fiber paper when compared with the bare papers even at lower air stoichiometry. The authors supposed that the MPL facilitates the back diffusion of water from the cathode through the membrane to the anode.

Extensive experimental works on the MPL have been performed by many researchers to investigate the effects of carbon powder type [9,10], PTFE content [11,12] and pore-forming agents [13,14] on the PEM fuel cell performance. Passalacqua et al. [10] prepared the MPLs by using different types of carbon blacks in order to clarify the effect of porous carbon structure on the fuel cell performance. They showed that the MPL prepared with Shawinigan acetylene black led to a better fuel cell performance when compared to the MPLs made using Asbury graphite 850, Mogul L and Vulcan XC-72. The observed performance improvement was attributed to higher pore volume and smaller pore size of acetylene black which facilitates the gas diffusion and also reduces the amount of water accumulation inside the MPL. Giorgi et al. [12] investigated how the PTFE content in the microporous layer affects the fuel cell performance. They suggested that 10 wt% PTFE as a binder in the microporous layer was required to avoid water flooding and to improve the gas transport. Kong et al. [13] made an attempt to modify the porous structure of the MPL by employing Li_2CO_3 as a pore-

* Corresponding author. Tel.: +1 803 777 7314; fax: +1 803 777 8265.
E-mail address: popov@engr.sc.edu (B.N. Popov).

0378-7753/$ – see front matter © 2006 Elsevier B.V. All rights reserved.
doi:10.1016/j.jpowsour.2006.09.020

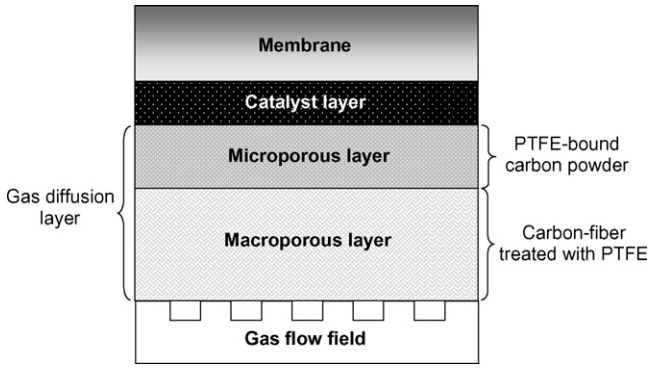

Fig. 1. Schematic diagram of a GDL for PEM fuel cell.

forming agent. They showed that when the pore-forming agent was removed with an aqueous H_2SO_4 solution, the volume of macropores (5–10 μm) increased, resulting in better fuel cell performance due to the reduced mass transport limitation in the MPL.

Williams et al. [3] estimated various physical parameters of the GDLs coated with the MPLs, such as: in-plane electronic resistivity, hydrophobicity, gas permeability and pore size distribution. The authors claim that the gas permeability is the most critical parameter which determines the oxygen limiting current when air is used as an oxidant. On the basis of the assumption that the water condensation occurs severely in pores smaller than 0.1 μm, it was experimentally shown that the GDL with higher gas permeability had smaller volume of water-saturated pores in the MPL which resulted in higher limiting currents.

Recent simulation studies [15,16] provided a fundamental understanding of how the MPL controls the water management and hence the fuel cell performance. From the viewpoint of water management, Weber and Newman [16] proposed that the MPL acts as a valve that pushes water away from the GDL to the flow field to minimize water flooding. They also made an attempt to optimize the MPL structures such as the hydrophobic property, bulk porosity, thickness and carbon loading.

The objective of the present work is to study the effect of carbon loading in the MPL on the PEMFC performance. The MPLs were prepared with different carbon loadings on the carbon-fiber substrate. Their porous structures were analyzed using mercury porosimetry. The fuel cell performances and ac-impedance spectra were evaluated with H_2/air. The goal was to understand the carbon loading effect on the oxygen diffusion and water management.

2. Experimental

2.1. Preparation of microporous layer on the carbon-fiber substrate

In order to prepare carbon ink for the MPL, carbon powder (0.4 g, acetylene black) was mixed with PTFE-dispersed water (60 wt% PTFE, Alfa Aesar), isopropyl alcohol (25 mL) and glycerol (0.8 mL) in an ultrasonic bath for 2 h. The resulting carbon ink was spray-deposited onto one side of the carbon-fiber paper pre-treated with 10 wt% PTFE (SGL 10CA, SGL Carbon Group), followed by drying at 80 °C for 30 min. The GDL sample was heat-treated at 280 °C for 30 min to evaporate all remaining glycerol, and then at 350 °C for 30 min to uniformly distribute PTFE throughout the MPL. In the MPL, the carbon loading and the PTFE content were varied between 0.2 and 2.0 mg cm^{-2} and between 6 and 40 wt%, respectively.

2.2. Physical characterization of gas diffusion layer

Porous structures of the GDL were characterized by using a mercury porosimeter (Micrometrics Autopore 9400). PSD curve was determined from the mercury intrusion data, i.e. the volume of mercury penetrating the pores versus the applied pressure p. Under the assumption that all pores are cylindrical, the pore diameter d_p was calculated from the value of p using a well-known capillary law [17]:

$$d_p = \frac{4\gamma \cos\theta}{p} \quad (1)$$

where γ and θ denote the surface tension of mercury and the contact angle of mercury with the sample, respectively.

2.3. Preparation of membrane-electrode assembly

The cathode catalyst ink was prepared by ultrasonically blending Pt/C powder (45 wt% Pt, Tanaka) with Nafion solution (5 wt% Nafion, Alfa Aesar), deionized water and methyl alcohol for 2 h. The catalyst ink was sprayed onto one side of the Nafion 112 membrane, followed by drying at 80 °C for 2 min. The process was repeated until a total Pt loading of 0.4 mg cm^{-2} was achieved. A commercially available catalyzed GDL (20 wt% Pt/C, 0.4 mg cm^{-2} Pt, E-TEK) was used as the anode for all fuel cell tests. A thin layer of Nafion (1.2 mg cm^{-2}) was coated on the anode surface to improve the adhesion between the catalyst layer and the membrane. The Nafion-coated anode was hot-pressed to the uncatalyzed side of the membrane at 140 °C and at 50 atm for 90 s. Finally, the GDL of interest was placed on the cathode catalyst layer.

2.4. Electrochemical measurements

The electrochemical experiments were carried out in a single cell with serpentine flow channels. Pure hydrogen gas humidified at 77 °C and air humidified at 75 °C were supplied to the anode and cathode compartments, respectively. All the measurements were performed at 75 °C and at ambient pressure.

Polarization technique was conducted with a fully automated test station (Fuel Cell Technologies Inc.) under the constant stoichiometry mode using a 30 mV potential step and a 5 min dwell time. The air stoichiometry λ_{air} and the geometric area of the MEA used were 2.0 and 25 cm^2, respectively. The electrochemical impedance spectroscopy (EIS) was performed under the constant flow rate mode by applying an ac-amplitude of 10 mV peak-to-peak over the frequency range from

Table 1
Pore characteristics of the GDLs as a function of carbon loading in the MPL, measured with a mercury porosimetry

Carbon loading (mg cm^{-2})	Average pore diameter, d_{avg} (μm)	Total pore volume, V_{total} (cm^3 g^{-1})
0	16.8	3.5
0.2	5.9	3.1
0.5	3.2	3.1
1.0	1.5	2.8
1.5	1.1	2.9
2.0	0.7	2.8

10 mHz to 10 kHz. The measurements were made at different cell potentials (E_{cell} = 0.4–0.9 V) and air flow rates (v_{air} = 20–60 mL min^{-1} cm^{-2}).

3. Results and discussion

Table 1 lists the average pore diameter d_{avg} and the total pore volume V_{total} in the GDLs as a function of carbon loading. The pore diameters and the pore volume V_{total} were estimated from the analyses of mercury intrusion data. The results indicated that when the MPL is deposited on the carbon-fiber substrate, d_{avg} reduces and gradually decreases with increasing the carbon loading. It is also noted that V_{total} decreases slightly when the MPL is present. This indicates that part of the MPL becomes entrenched into the carbon-fiber substrate during the spray-deposition of carbon ink.

Fig. 2 shows the PSD curves (dV/dd_p) for the GDLs as a function of carbon loading in the MPL. Also, the PSD curve of bare carbon-fiber substrate is given in Fig. 2. Comparing the PSD data for the GDLs with and without the MPL, it is clear that the pore size ranges between 0.02 and 0.5 μm in the MPL and from 20 to 100 μm in the carbon-fiber substrate. The differential pore volume in the MPL increases with the carbon loading, while the PSD remains almost unchanged in the carbon-fiber substrate (see the inset).

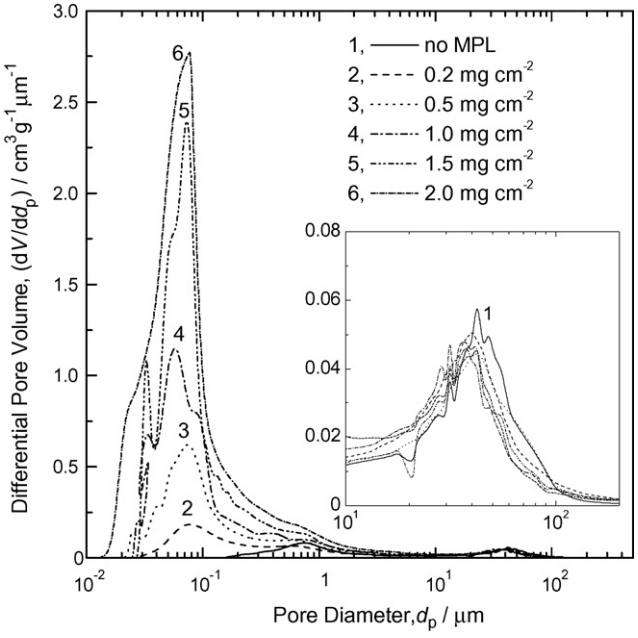

Fig. 2. PSD curves (dV/dd_p) for the GDLs as a function of carbon loading in the MPL.

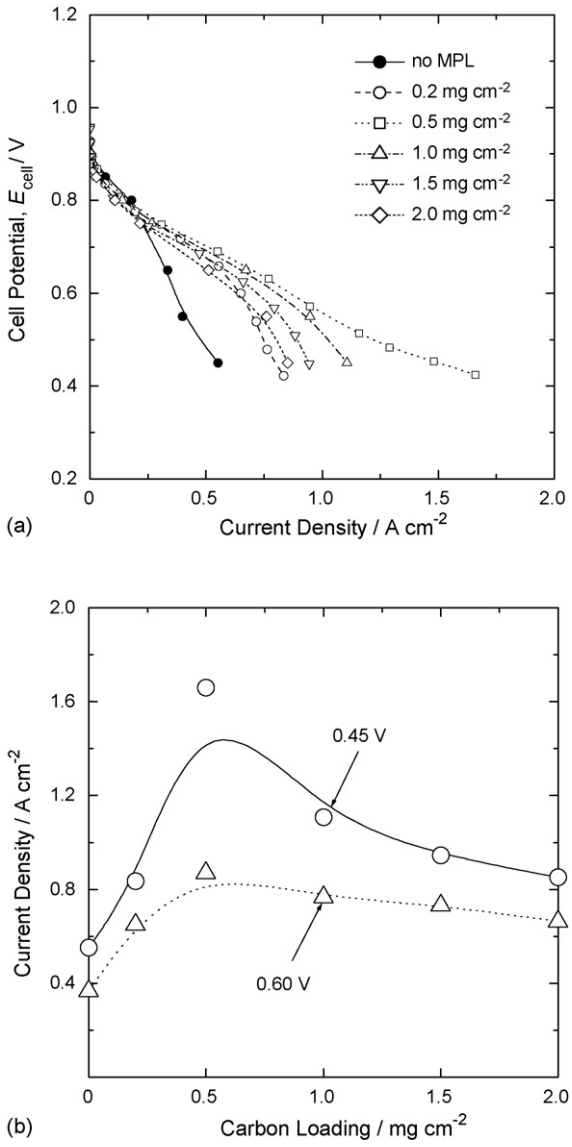

Fig. 3. (a) Polarization curves of PEMFCs and (b) current densities at 0.45 and 0.6 V as a function of carbon loading in the MPL. The experiments were performed under the constant stoichiometry mode of λ_{air} = 2.0.

Fig. 3(a) illustrates polarization curves of the PEMFCs measured using the MPLs loaded with different amounts of carbon. The experiments were performed with H_2/air under the constant stoichiometry mode of λ_{air} = 2.0. The polarization curve obtained using no MPL was also presented in Fig. 3(a) for comparison. Fig. 3(a) shows that the use of the MPLs results in the improved fuel cell performance and the improvement is highly dependent upon the carbon loading in the MPL. The current densities determined at 0.45 and 0.6 V are presented in Fig. 3(b) as a function of carbon loading. The fuel cell performance reaches a maximum for 0.5 mg cm^{-2}, and then the performance decays with further increasing the carbon loading. This experimental result agrees qualitatively with the recent simulation study of

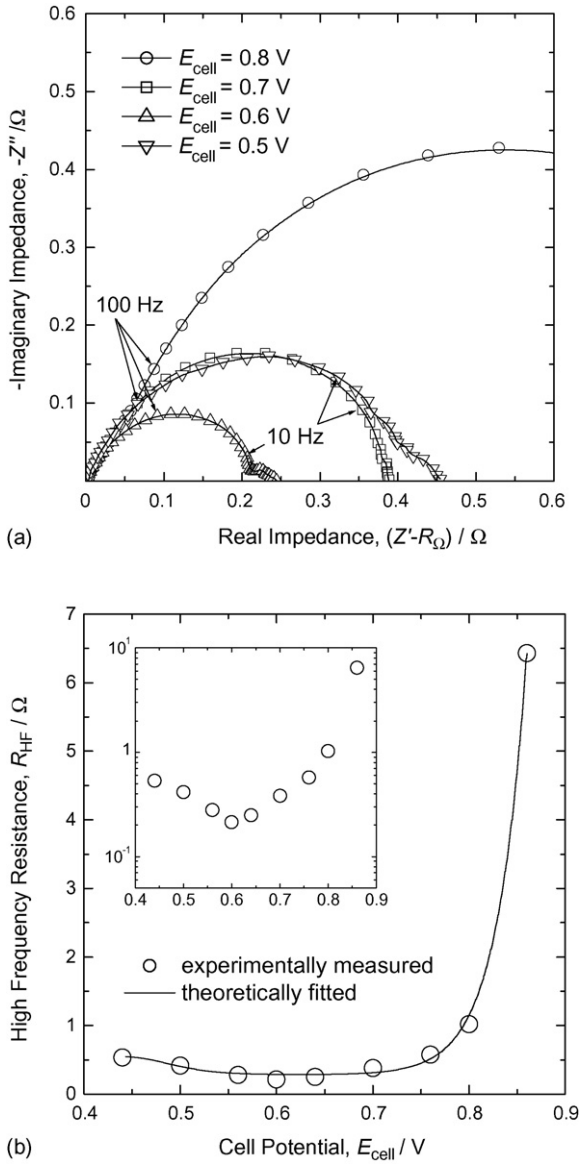

Fig. 4. (a) Nyquist plots of the ac-impedance spectrum measured at various values of E_{cell} and (b) the dependence of R_{HF} on E_{cell}. The experiments were performed using the MPL loaded with 0.5 mg cm^{-2} carbon under the constant flow rate mode of v_{air} = 60 mL min^{-1} cm^{-2}.

Weber and Newman [16] who demonstrated the best fuel cell performance is observed with a relatively thin MPL (i.e. low carbon loading).

The experimental PSD and polarization data in this study indicate that a high volume of micropores in the GDL is not a necessary condition for achieving a high fuel cell performance: namely, there exists an optimum micropore volume or carbon loading for effective transport of gaseous oxygen and liquid water inside the MEA.

The analysis of the ac-impedance behavior may provide the useful information to understand how the micropores control the fuel cell performance, since the EIS technique allows to separately study electrode processes with different relaxation times. Fig. 4(a) shows typical Nyquist plots of the ac-impedance spectrum measured on the PEMFC at different values of E_{cell}. The measurements were conducted using the MPL loaded with 0.5 mg cm^{-2} carbon under the constant flow rate mode of v_{air} = 60 mL min^{-1} cm^{-2}. In order to restrict our discussion to the interfacial reactions and mass transport in the PEMFC, the measured real impedance Z' was subtracted by the ohmic resistance R_Ω in Fig. 4(a). At high potentials above 0.6 V, the ac-impedance spectrum shows only a depressed arc over the whole frequency range. On the other hand, a two-arc behavior is observed with an additional arc in the low frequency range below 0.6 V. The magnitude of high-frequency arc, R_{HF}, was determined from the ac-impedance spectrum using a complex non-linear least squares (CNLS) method, and plotted in Fig. 4(b) as a function of E_{cell}. R_{HF} decreases to a minimum value with lowering E_{cell} from 0.85 to 0.6 V, and then it rises slowly when E_{cell} becomes lower than 0.6 V. The experimental potential-dependence of R_{HF} shown in Fig. 4(b) has been also observed by other researchers [18,19], and can be satisfactorily interpreted in terms of the 'thin film/flooded-agglomerate model' of catalyst layer [20,21].

The model assumes that the catalyst layer consists of (i) porous agglomerates of the polymer electrolyte (Nafion) and the carbon-supported Pt particles and (ii) the macropores through which gaseous oxygen diffuses. The macropores are partially flooded with a thin film Nafion electrolyte which has hydrophobic microporous channels. Oxygen diffuses through such hydrophobic channels towards the catalyst particles in the agglomerates, and then charge transfer reaction takes place at the three-phase boundaries.

The ac-impedance response of agglomerate dynamics combined with thin film diffusion has been theoretically well-established, and a simple analytical equation was derived for R_{HF} as follows [19–21]:

$$\frac{R_{HF}}{R_0} = \frac{2[1 + \Gamma e^{\mu}\{(\tanh \Phi e^{\mu/2})/\Phi e^{\mu/2}\}]}{[\mathrm{sech}^2 \Phi e^{\mu/2} + \{(\tanh \Phi e^{\mu/2})/\Phi e^{\mu/2}\}]e^{\mu/2}} \quad (2)$$

with

$$\mu = \frac{\alpha F}{RT}\eta \quad (3)$$

$$\Phi = \left(\frac{L_y k_0}{D_a}\right)^{1/2} \quad (4)$$

$$\Gamma = \frac{\delta k_0}{D_f} \quad (5)$$

where μ is the dimensionless overpotential, Φ and Γ are the parameters characterizing the agglomerate and thin film diffusion processes, respectively, and R_0 represents the resistance value at $\mu = 0$ in the absence of mass transport limitations ($\Phi \to 0$ and $\Gamma \to 0$). α is the transfer coefficient, F the Faraday constant, η the cathodic overpotential, R the gas constant, T the absolute temperature, k_0 the rate constant for charge transfer, L_y and δ the thickness of the agglomerate layer and that of the thin electrolyte film, respectively, and D_a and D_f symbolize the diffusion coefficients of oxygen in the agglomerate and in the thin electrolyte film, respectively.

According to Eq. (2), depending on the cathodic overpotential, interfacial charge transfer is kinetically coupled with

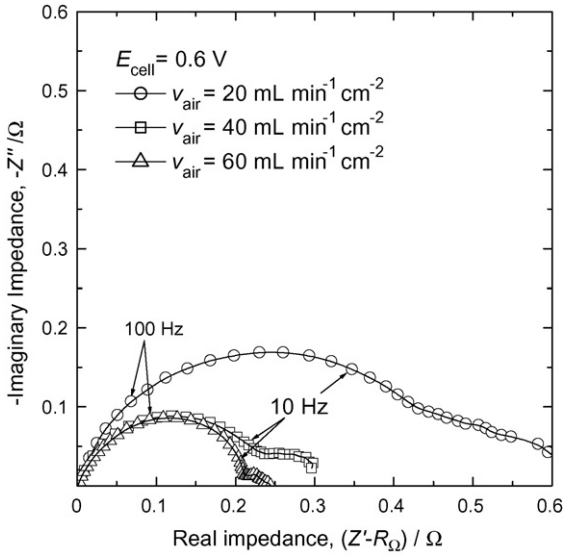

Fig. 5. ac-Impedance spectra measured at 0.6 V as a function of v_{air}. The experiments were performed using the MPL loaded with 0.5 mg cm^{-2} carbon.

different diffusion processes: (i) oxygen diffusion through the agglomerate pores (agglomerate diffusion) and (ii) oxygen diffusion through the thin Nafion layer (thin film diffusion). For low μ values, the agglomerate diffusion process is dominant and R_{HF} continuously decreases with increasing μ. In contrast, for high μ values, the thin film diffusion becomes non-negligible and thus R_{HF} rises with increasing μ.

As shown in Fig. 4(b), the experimental R_{HF} versus E_{cell} plot can be fitted quite well to Eq. (2) by taking the values of Φ and Γ as 3.8×10^{-4} and 4.7×10^{-4}, respectively. This confirms that thin film/flooded-agglomerate dynamics in the catalyst layer is responsible for a high-frequency arc in the ac-impedance spectrum. Especially, the appearance of a turnaround potential of 0.6 V at which R_{HF} starts increasing, indicates that the electrode kinetics is controlled by agglomerate diffusion above 0.6 V, while thin film diffusion acts as a rate-determining step below 0.6 V.

It is of great importance to note that the ac-impedance spectrum in Fig. 4(a) exhibits an additional arc in the low frequency range at E_{cell} lower than 0.6 V. Various models have been proposed to explain the appearance of such a low-frequency arc, including: (i) oxygen diffusion through the GDL [18,19], (ii) back diffusion of water in the membrane [22] and (iii) water diffusion in the catalyst layer [23].

In this study, the ac-impedance spectrum was measured at 0.6 V as a function of v_{air} in order to figure out the origin of the low-frequency arc, and the results are given in Fig. 5. It is clearly seen that the magnitude of the low-frequency arc, R_{LF}, increases with decreasing v_{air}. Since water diffusion in the membrane and the catalyst layer essentially remains unaffected by v_{air} [19], the dependence of R_{LF} on v_{air} suggests that slow oxygen diffusion in the GDL is responsible for R_{LF}. That is, the lower the value of v_{air} is, the larger is the concentration gradient of oxygen across the GDL, and thus the larger is the value of R_{LF}. Also, from the fact that R_{LF} strongly depends on the GDL thickness or cathode humidification, Springer et al. [18] and Ciureanu and Roberge [19] have concluded that the low-frequency arc in their impedance data is caused by oxygen diffusion through the GDL.

For the ternary gas system (oxygen, nitrogen and water vapor), Springer et al. [18] formulated the theoretical expressions for impedance response resulting from the oxygen diffusion reaction through the GDL. An approximate analytical solution follows the form of the impedance equation for thin-film diffusion which is frequently called the Gerischer behavior: the ac-impedance spectrum should exhibit a straight line inclined at a constant angle of 45° to the real axis, followed by an arc. However, such a straight line was not clearly observed in Fig. 5 due to the interference with high-frequency arc. The increasing tendency of R_{HF} with decreasing v_{air} may be explained in terms of the slower interfacial reaction in the catalyst layer as a result

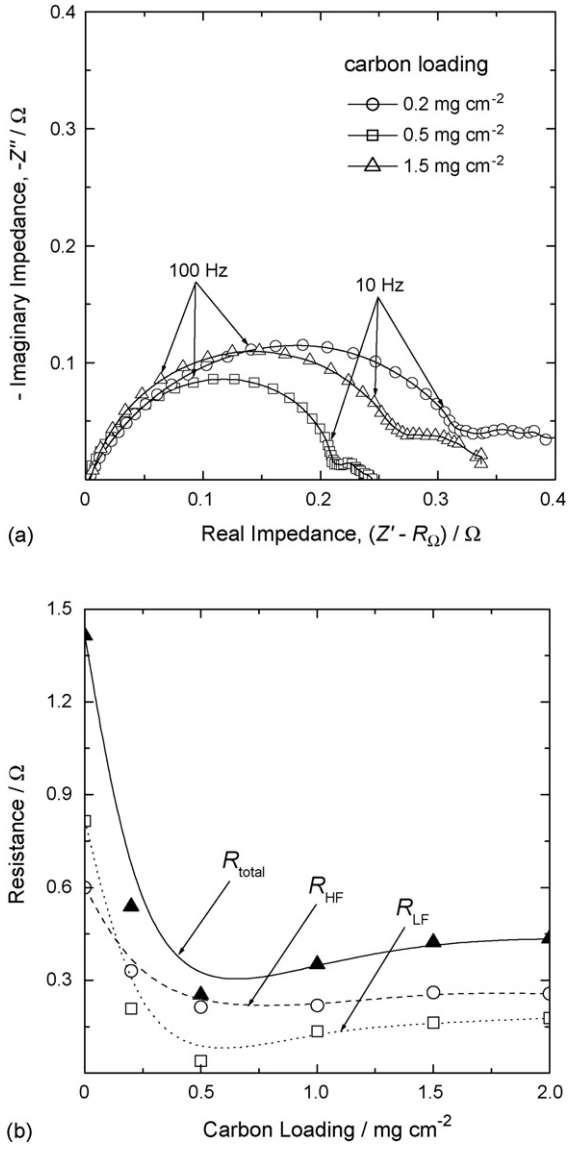

Fig. 6. (a) Nyquist plots of the ac-impedance spectrum as a function of carbon loading in the MPL and (b) the dependences of R_{HF} and R_{LF} on the carbon loading. The experiments were performed at 0.6 V under the constant flow rate mode of $v_{air} = 60$ mL min^{-1} cm^{-2}.

of oxygen diffusion limitation in the GDL. It appears that at high overpotentials, excess water accumulated in the GDL may significantly inhibit oxygen diffusion by decreasing the GDL porosity. In fact, the low-frequency arc is only observed below 0.6 V, as shown in Fig. 4(a).

Fig. 6(a) illustrates the Nyquist plots of the ac-impedance spectrum as a function of carbon loading in the MPL. The spectra were measured at 0.6 V with $v_{air} = 60\,mL\,min^{-1}\,cm^{-2}$. All of the ac-impedance spectra consist of two separated arcs, but the values of R_{HF} and R_{LF} strongly depend on the carbon loading. As demonstrated in Fig. 6(b), the MPL loaded with 0.5 mg cm^{-2} carbon results in a minimum value of R_{total} ($=R_{HF}+R_{LF}$), indicating the enhanced kinetics of oxygen diffusion in both the catalyst layer and the GDL.

At this point, it should be noted that the pores sizes in the MPL are smaller by about three orders of magnitude than those in the carbon-fiber substrate, as illustrated in the PSD curves of Fig. 2. Therefore, the MPL may increase the resistance of water flow from the catalyst layer to the carbon-fiber substrate due to its smaller pores. In fact, our preliminary study on water management showed that the liquid water permeability is reduced by more than one order of magnitude when the MPL is deposited onto the carbon-fiber substrate. The detailed results of water permeation experiments will be presented in the following paper. Thus, high levels of carbon loading (or micropore volume) in the MPL cause severe water flooding in the catalyst layer due to high flow resistance in the MPL, thereby inhibiting agglomerate diffusion. By contrast, low levels of carbon loading (or micropore volume) in the MPL results in water flooding in the carbon-fiber substrate, thereby impeding oxygen diffusion in the GDL. The polarization and ac-impedance experiments in this study indicate that the MPL loaded with 0.5 mg cm^{-2} carbon results in an effective water management, viz. a balancing of water saturations in the catalyst layer and the GDL, and hence enhances the oxygen diffusion kinetics and the PEMFC performance.

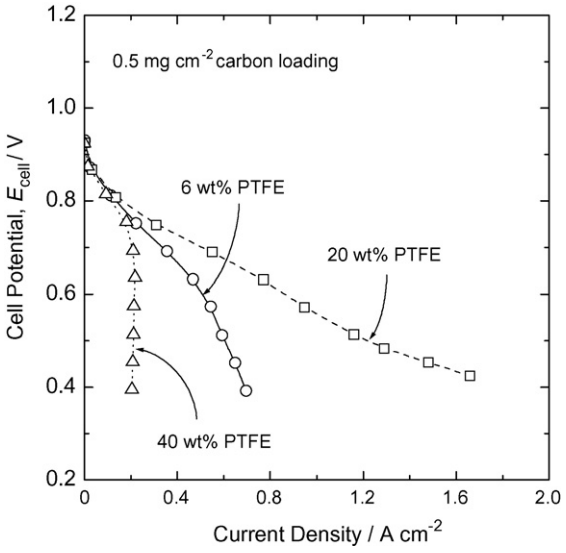

Fig. 7. Polarization curves of the PEMFCs measured using the MPLs with different PTFE contents. The experiments were performed using the MPL loaded with 0.5 mg cm^{-2} carbon under the constant stoichiometry mode of $\lambda_{air} = 2.0$.

Fig. 7 exhibits polarization curves of the PEMFCs measured using the MPLs with different PTFE contents. The experiments were performed with H_2/air under the constant stoichiometry mode of $\lambda_{air} = 2.0$. The 20 wt% PTFE-containing MPL leads to better PEMFC performance as compared to those with 6 and 40 wt% PTFE. Similarly to the case of carbon loading effect, the observed polarization behavior can be explained as follows: for 40 wt% PTFE content, the resistance for water flow may be significantly high due to a large volume of hydrophobic pores in the MPL. This results in severe water flooding in the catalyst layer. On the contrary, the 6 wt% PTFE content results in water flooding in the carbon-fiber substrate. Also, it is plausible that most of the micropores are flooded with water, since the PTFE content in the MPL is even less than that in the carbon-fiber substrate.

4. Conclusion

The microporous layers were prepared with different carbon loadings on the carbon-fiber substrates, and their porous structures were characterized by using mercury porosimetry. Polarization experiments showed that when air was used as an oxidant, the microporous layer loaded with 0.5 mg cm^{-2} carbon resulted in the best fuel cell performance. From the dependences of the ac-impedance spectra on the cell potential and air flow rate, the impedance properties were analyzed in terms of the thin film/flooded-agglomerate dynamics in the catalyst layer and oxygen diffusion in the GDL. The ac-impedance study indicated that the optimized microporous layer results in an effective water managements, i.e. a balancing of water saturations in the catalyst layer and the GDL.

Acknowledgment

Financial support provided by Fuji Photo Film Inc. is acknowledged gratefully.

References

[1] E.R. Gonzalez, S. Srinivasan, Int. J. Hydrogen Energy 9 (1984) 215–218.
[2] M.C. Williams, Fuel Cell Handbook, 6th ed., 2002.
[3] M.V. Williams, E. Begg, L. Bonville, H.R. Kunz, J.M. Fenton, J. Electrochem. Soc. 151 (2004) A1173–A1180.
[4] A. Fischer, J. Jindra, H. Wendt, J. Appl. Electrochem. 28 (1998) 277–282.
[5] M.S. Wilson, J.A. Valerio, S. Gottesfeld, Electrochim. Acta 40 (1995) 355–363.
[6] L.R. Jordan, A.K. Shukla, T. Behrsing, N.R. Avery, B.C. Muddle, M. Forsyth, J. Power Sources 86 (2000) 250–254.
[7] Z. Qi, A. Kaufman, J. Power Sources 109 (2002) 38–46.
[8] G. Lin, T.V. Nguyen, J. Electrochem. Soc. 152 (2005) A1942–A1948.
[9] L.R. Jordan, A.K. Shukla, T. Behrsing, N.R. Avery, B.C. Muddle, M. Forsyth, J. Appl. Electrochem. 30 (1999) 641–646.
[10] E. Passalacqua, G. Squadrito, F. Lufrano, A. Patti, L. Giorgi, J. Appl. Electrochem. 31 (2001) 449–454.
[11] F. Lufrano, E. Passalacqua, G. Squadrito, A. Patti, L. Giorgi, J. Appl. Electrochem. 29 (1999) 445–448.
[12] L. Giorgi, E. Antolini, A. Pozio, E. Passalacqua, Electrochim. Acta 43 (1998) 3675–3680.
[13] C.S. Kong, D.-Y. Kim, H.-K. Lee, Y.-G. Shul, T.-H. Lee, J. Power Sources 108 (2002) 185–191.

[14] Y. Song, Y. Wei, H. Xu, M. Williams, Y. Liu, L.J. Bonville, H.R. Kunz, J.M. Fenton, J. Power Sources 141 (2005) 250–257.
[15] U. Pasaoqullari, C.Y. Wang, J. Electrochem. Soc. 151 (2004) A399–A406.
[16] A.Z. Weber, J. Newman, J. Electrochem. Soc. 152 (2005) A677–A688.
[17] A.W. Adamson, A.P. Gast, Physical Chemistry of Surfaces, 6th ed., Wiley, Chichester, 1997, p. 784.
[18] T.E. Springer, T.A. Zawodzinski, M.S. Wilson, S. Gottesfeld, J. Electrochem. Soc. 143 (1996) 587–599.
[19] M. Ciureanu, R. Roberge, J. Phys. Chem. B 105 (2001) 3531–3539.
[20] T.E. Springer, I.D. Raistrick, J. Electrochem. Soc. 135 (1989) 1594–1603.
[21] I.D. Raistrick, Electrochim. Acta 25 (1990) 1579–1586.
[22] V.A. Paganin, C.L.F. Oliveira, E.A. Ticianelli, T.E. Springer, E.R. Gonzalez, Electrochim. Acta 43 (1998) 3761–3766.
[23] N. Wagner, W. Schnurnberger, B. Müller, M. Lang, Electrochim. Acta 43 (1998) 3785–3793.